



Theoretical and experimental study of cephalexin batch adsorption dynamics using walnut shell-based activated carbon

Ghadir Nazari^a, Hossein Abolghasemi^{a,b,*}, Mohamad Esmaili^a, Moein Assar^a

^aCenter for Separation Processes Modeling and Nano-Computations, School of Chemical Engineering, College of Engineering, University of Tehran, P.O. Box 11365-4563, Tehran, Iran, Tel. +98 21 61112186; Fax: +98 21 66954051;

emails: ghadir_nazari@alumni.ut.ac.ir, ghadir_nazari@yahoo.com (G. Nazari), hoab@ut.ac.ir, Abolghasemi.ha@gmail.com (H. Abolghasemi), esmaili@ut.ac.ir (M. Esmaili), assar.engbox@gmail.com (M. Assar)

^bOil and Gas Center of Excellence, University of Tehran, Tehran, Iran

Received 22 September 2015; Accepted 22 March 2016

ABSTRACT

Batch adsorption of cephalexin (CFX) by walnut shell activated carbon is studied both experimentally and mathematically. Firstly, the adsorbent was prepared by chemical activation method in the presence of $ZnCl_2$. Next, the values of adsorbent dosage and pH were optimized. Then, the effect of initial CFX concentration and contact time was studied to evaluate the kinetics and the equilibrium isotherm. It is found that the Freundlich and Toth models provided the best fit to the experimental data. Dynamic characteristics of this process are mathematically modeled. In the developed model, pore diffusivity is estimated according to the experimental results. The model reveals good agreement with experiment. The effective diffusivity of CFX in the walnut shell AC is estimated as $0.47 \times 10^{-9} \text{ m}^2 \text{ s}^{-1}$.

Keywords: Adsorption; Batch modeling; Cephalexin; Activated carbon; Diffusivity estimation

1. Introduction

Chemicals are used everyday in homes, industry, hospital, and agriculture, and can be released to the environment as wastewater effluents. These chemicals include various materials such as human and veterinary drugs. A vast array of pharmaceuticals—including antibiotics, are being detected in the environment and there is genuine concern that these compounds, in the small concentrations that they're at, could be causing impacts to human health or to aquatic organisms. Due to the prevalence of their respective antibiotic family usage, cephalexin (CFX) was selected as an adsorbate for adsorption process in this work. The

CFX is in a group of drugs called cephalosporin antibiotics and is used to treat a number of infections in the body. Some technologies like reverse osmosis [1], ozonation and biomembrane [2], and biological filtration technologies [3] can be applied to remove such compounds during the wastewater treatment process. However, they are very expensive and rarely used. Adsorption is a simple and affordable method for the removal of drug compounds from water and wastewater. Drug adsorption has been studied by different adsorbent such as silica [4], single-walled and multi-walled carbon nanotube [5], kaolinite [6], bamboo charcoal [7], and montmorillonite [8]. Activated carbon (AC) [9–12] and polymeric resins [13] have been suggested for the adsorption of CFX from aqueous solutions. The cost of adsorption process strongly depends

*Corresponding author.

on the manufacturing cost of the adsorbent. ACs are among classic adsorbents for the removal of a wide range of contaminations. Nowadays, it is common practice to prepare AC from low-priced material such as agriculture waste [14–17]. In this regard, the performance of the AC adsorbent obtained from walnut shell, as an inexpensive precursor, has been studied for the removal of CFX in a batch process. Adsorption processes are studied mathematically using various mathematical representations, each basically trying to improve the predictions. External film diffusion model, intraparticle diffusion model, film-surface diffusion model, and film-pore diffusion model are all examples of such attempts [18,19]. As a result of non-linearity of the governing equations, explicit analytical solutions are difficult or impossible to derive, except for simplified cases such as linear isotherm [20–23]. Several solution methods have been specifically applied to batch adsorption processes. The collocation algorithm, finite difference algorithm, the matrix multiplicative weights update model (MMW), integral formulation method, and the weighted arithmetic mean method (WAMM) are among the numerical methods that are frequently used [24,25]. If separation phenomena are accurately described through the development of mathematical formulations, such formulations will be useful in the design and optimization of processes in any operating units. In this regard, the knowledge of the dynamic diffusion radius is of fundamental importance for the mathematical modeling and engineering design of adsorption process. The point is that there is no known experimental method to obtain the radius of diffusion dynamically. Our best literature reviews demonstrate that there is no study regarding the diffusion radius of antibiotics like CFX through the AC pores. For the purpose mentioned above, i.e. the dynamic modeling of diffusion radius, a pore diffusion-based model was developed. In order to solve the obtained differential equation, the implicit finite difference method of line, a numerical method, was applied. The advantage of this method is its simplicity and accuracy at the same time. The purpose of this research involved two sections. In the first section, preparation of AC from the walnut shell for the batch adsorption of CFX in an aqueous solution was investigated. Afterwards, the kinetics and the equilibrium isotherm of the process at the optimized values of initial solution pH and adsorbent dosage were obtained at a constant temperature of 30°C. Then, the experi-

mental equilibrium isotherm was modeled using the Langmuir, the Freundlich, the Sips, and the Toth models. In the second section, for mathematical investigation of the batch adsorption process, a pore diffusion model is developed. Implicit finite difference method of line is applied to handle the mathematical problem. Finally, the model is successfully used as a mean to evaluate the effective diffusivity of CFX in the adsorbent. In this study, used rate equation was based on the pore diffusion mechanism. Our recommendations for future researches are: (1) to consider other mechanisms like solid diffusion, parallel pore and solid diffusion, and also diffusion in bidispersed particles and (2) to employ the developed model in this study in the adsorption of other similar antibiotics in structure onto other similar adsorbents.

2. Mathematical modeling

As previously mentioned, mathematical representation is based on the film-pore diffusion model. The following assumptions are made to develop the model:

- (1) Constant temperature throughout the adsorption process.
- (2) Since stirring rate is high, the external mass transfer resistance is assumed to be negligible in comparison with pore diffusion one.
- (3) In the whole of adsorbent, pore concentration is at total equilibrium with solid concentration.
- (4) All the particles are sphere.

2.1. Equilibrium condition

Over time, the system approaches equilibrium state. Overall mass balance at equilibrium state is expressed by (Eq. (1)):

$$C_{b,0}V = C_eV + q_eW \quad (1)$$

where $C_{b,0}$ is the bulk phase concentration at initial condition, C_e and q_e are the equilibrium concentration and adsorption capacity, respectively. Also, V is the volume of liquid solution and W indicates the adsorbent weight. C_e and q_e can be calculated by simultaneous solution of Eq. (1) and the equilibrium isotherm. Eq. (2) can be obtained by means of the Langmuir isotherm:

$$C_e = \frac{V(C_{b,0}K_L - 1) - Q_0K_LW + \sqrt{(V(1 + C_{b,0}K_L) + K_LWQ_0)^2 - 4b^2WQ_0VC_{b,0}}}{2K_LV} \quad (2)$$

where K_L is the Scherrer constant. The more complicated isotherm models can also be handled numerically.

2.2. Solid phase

The Eq. (3) holds for an adsorbent grain based on Fick’s law of diffusion and according to Fig. 1:

$$\varepsilon_p \frac{\partial C_p}{\partial t} = D_e \frac{1}{r^2} \frac{\partial}{\partial r} \left(r^2 \frac{\partial C_p}{\partial r} \right) - \rho_s (1 - \varepsilon_p) \frac{\partial q}{\partial t} \tag{3}$$

where ε_p is the adsorbent porosity, D_e is the effective diffusivity, C_p is the pore concentration in the liquid phase, q is the adsorption capacity, r is the radial coordinate for the grain, and t indicates the time. Also, ρ_s shows the skeletal density. In this model, the moisture diffuses in the pores from the surface toward the center and adsorbs gradually on the adsorbent. At any radius, equilibrium is assumed to be instantaneously established on the grain surface. The Eq. (3) can be rearranged to form the following nonlinear equation (Eq. (4)):

$$\frac{\partial C_p}{\partial t} = \frac{D_e}{\left[\varepsilon_p + \rho_s (1 - \varepsilon_p) \frac{\partial q}{\partial C_p} \right]} \frac{1}{r^2} \frac{\partial}{\partial r} \left(r^2 \frac{\partial C_p}{\partial r} \right) \tag{4}$$

The term $\partial q / \partial C_p$ is derived from equilibrium isotherm and forms the nonlinear term of Eq. (4).

Boundary conditions can be expressed by the following equations (Eqs. (5) and (6)):

$$\frac{\partial C_p(0, t)}{\partial t} = 0 \tag{5}$$

$$C_p(R_p, t) = C_b(t) \tag{6}$$

while the initial conditions read as (Eqs. (7) and (8)):

$$C_p(r, 0) = 0 \tag{7}$$

$$C_b(0) = C_{b,0} \tag{8}$$

2.3. Bulk liquid phase

Bulk concentration decreases as the adsorbate adsorbs on the adsorbent particles. Establishment of mass balance leads to the below equation (Eq. (9)):

$$V \frac{dC_b}{dt} = -NAD_e \frac{\partial C_p(R, t)}{\partial r} \tag{9}$$

where A is the external area of a grain and N is the number of adsorbent grains and calculates as (Eq. (10)):

$$N = \frac{W}{\frac{4}{3} \pi R^3 \rho_s (1 - \varepsilon_p)} \tag{10}$$

3. Numerical analysis of the model

As mentioned before, numerical solution is based on the implicit finite difference method of line. A MATLAB (MathWorks Inc., Natick, MA) code was developed to perform the calculations. Eqs. (4) and (9), were fully discretized. For elaboration, these equations are discretized as:

$$\frac{dC_{p,(i)}}{dt} = Q_{(i)} \left(\frac{C_{p,(i+1)} - 2C_{p,(i)} + C_{p,(i-1)}}{\delta r^2} \right) + \frac{2Q_{(i)}}{r_i} \left(\frac{C_{p,(i+1)} - C_{p,(i-1)}}{2\delta r} \right) \tag{11}$$

$$\frac{dC_b}{dt} = -\frac{NAD_e}{V} \left(\frac{C_b - C_{p,(I-1)}}{\delta r} \right) \tag{12}$$

where δ_r is the increment in r-direction. Eqs. (11) and (12) are obtained by the central differentiation scheme for the internal nodes. For boundary nodes, boundary conditions are utilized together with either a forward or backward differentiation scheme. A system comprising I (number of discretized nodes) ODEs is formed. Utilizing the fourth-order Runge–Katta algorithm for each one of them implicitly formed a system of I nonlinear algebraic equations. The nonlinearity of the

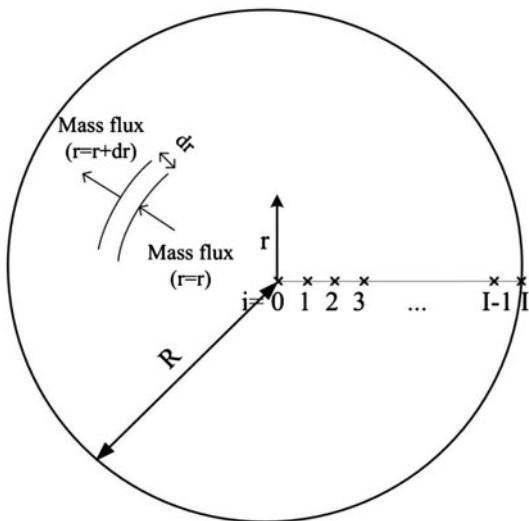


Fig. 1. Discretization of governing equation in a single adsorbent grain.

system can be handled by a trial-and-error loop. Since the grain concentration gradient is declining, varying time increments (δt) were used at different stages of simulation. They started from 0.01 to 5 s. The number of nodes was also chosen 50.

4. Materials and methods

4.1. Materials

In this study, walnut shell was used as the raw material. Its chemical analysis (% by weight) is listed as: cellulose = 38.7, Lignin = 24.7, hemicellulose = 18.4, extractable material = 7.5, ash = 2.6, and moisture = 8.1. Zinc chloride (ZnCl_2) was also supplied by Merck Company. The CFX antibiotic (supplied by LOGHMAN Pharmaceutical & Hygienic Co., Tehran, Iran) of purity 99.8% was used as an adsorbate. Table 1 shows the properties of CFX.

4.2. Preparation of walnut shell AC

Walnut shell was perfectly washed with distilled water for several times, dried, and then sieved to the particle size of 251–354 nm. For the production of AC, ZnCl_2 was dissolved in water and walnut shell (5 g) was added to the solution at 1–1 impregnation ratio (defined by the weight ratio of ZnCl_2 to walnut shell) and was stirred for 6 h. Then, the sample was put in an oven at 105°C until completely dried (24 h). The prepared sample was placed in a vertical stainless steel reactor (with length 100 cm and internal diameter 2.4 cm). Under high purity nitrogen (99.99%) flow rate of $300 \text{ cm}^3 \text{ min}^{-1}$, the sample was heated to a final temperature of 450°C with heating rate of 5°C min^{-1} . The sample was activated at the final temperature during 60-min holding time and then the sample slowly reached room temperature. Walnut shell AC dried completely in an oven at 105°C, then the sample was thoroughly washed with a 0.05 M HCl solution in order to remove the residual ZnCl_2 . The sample was washed with distilled water until it reached the pH value between 6 and 7. Finally, the sample was dried in an oven at 105°C for 24 h [26].

4.3. Characterization methods

The textual characterization of the walnut shell AC was carried out by N_2 adsorption at 77 K. The surface area was calculated from the isotherms using the Brunauer–Emmett–Teller (BET) equation. Total pore volume using nitrogen vapor adsorption data in the relative pressure of 0.95 and an average pore diameter using the Barrett–Joyner–Halenda (BJH) equation were determined. To study the surface functional groups in the spectral range 400–4,000 cm^{-1} , the Fourier transform infrared (FTIR) spectroscopy was used. Scanning electron microscopy (SEM) was applied for the morphological study of the samples.

4.4. Batch adsorption tests

The experiments were carried out in a set of 100-mL Erlenmeyer flasks where 50 mL of CFX aqueous solution was shaken with walnut shell AC at 200 rpm and at a constant temperature of 303 K. The initial pH of the solution was adjusted around 6.5 by the addition of a few droplets of 0.1 M HCl and 0.1 M NaOH solution. After equilibrium, the suspension was centrifuged and the concentration of CFX in liquid phase was determined by using a UV–vis spectrophotometer (UNICAM, 8700 series, USA) at a maximum wavelength of 263 nm. The amount of CFX adsorbed onto walnut shell AC was calculated as:

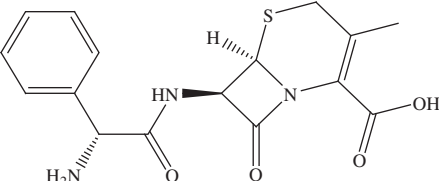
$$q_t = \frac{(C_0 - C_t)V}{W} \quad (13)$$

5. Results and discussion

5.1. Effect of adsorbent dosage

The optimum amount of adsorbent dosage was investigated using different amounts of the adsorbent (0.005–0.04 g) with 50 mL of 100 mg L^{-1} CFX solutions at an initial pH of 6.5 for 20 h. As illustrated in Fig. 2, the optimum walnut shell AC dose was evaluated to be 0.03 g of the adsorbent in 50 mL of the CFX

Table 1
Properties of CFX

Chemical structure	Molecular formula	Molecular weight (g mol^{-1})
	$\text{C}_{16}\text{H}_{17}\text{N}_3\text{O}_4\text{S}$	347.6

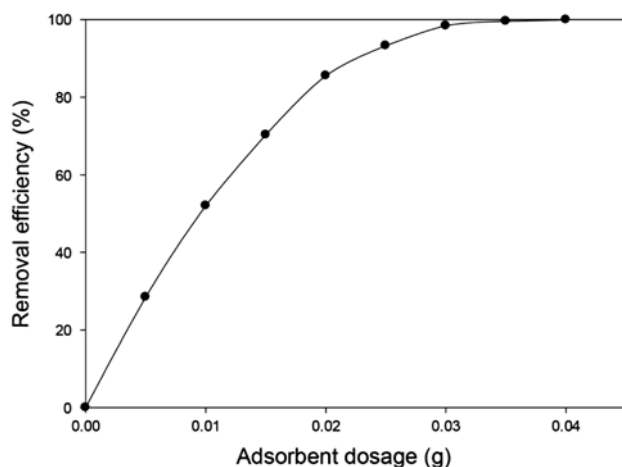


Fig. 2. Effect of adsorbent dosage on the removal efficiency of the CFX ($T = 30^\circ\text{C}$ and $C_0 = 150 \text{ mg L}^{-1}$).

solution. The increase in CFX uptake by increasing the adsorbent dose is attributed to many reasons, such as availability of solute, electrostatic interactions, and interference between binding sites. Thus, the adsorption sites remain unsaturated during the adsorption process due to a lower adsorptive capacity utilization of the sorbent, which decreases the adsorption efficiency [27]. As a result, the removal efficiency did not change dramatically after increasing the adsorbent dosage above 0.03 g.

5.2. Effect of initial solution pH

The initial solution pH study was carried out by contacting 0.03 g of walnut shell AC with 50 mL of 150 mg L^{-1} CFX solutions at different values of initial solution pH ranging from 1.5 to 8.5 for 20 h. As illustrated in Fig. 3, the maximum removal efficiency of the walnut shell AC occurs at an initial solution pH of 6.5. This trend can be justified by the pH_{pzc} of the adsorbent (the pH value at which the surface charge density is zero). The pH_{pzc} of the adsorbent was found to be 6.67 based on the method described by Reddy et al. [28]. The molecular structure of CFX and its ionic forms as a function of pH is shown in Fig. 4. At pH values less than 2.56, physisorption is thought to dominate the adsorption process. The reason can be the positively charged surface of the adsorbent at pH values less than the pH_{pzc} . The zwitterionic form of CFX molecules is predominant at pH values ranging from 2.56 to 6.88. As the pH value increases, the concentration of negatively charged CFX species in the solution bulk rises up. Therefore, both the chemi- and physisorption control the adsorption of CFX and the maximum adsorption capacity occurs at pH 6.5 as

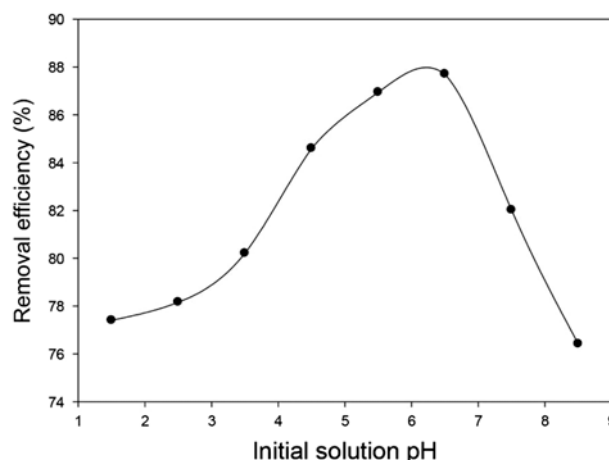


Fig. 3. Effect of pH on the removal efficiency of the CFX ($T = 30^\circ\text{C}$ and $C_0 = 150 \text{ mg L}^{-1}$).

219.25 mg g^{-1} . At pH values higher than 6.88, physisorption may be responsible for the adsorption of CFX because the surface of walnut shell AC at pH values higher than the pH_{pzc} is negatively charged.

5.3. Adsorption kinetics

The effect of contact time on the adsorption of CFX onto walnut shell AC was independently studied by contacting 0.03 g of the walnut shell AC with CFX solutions at different initial concentrations of 100, 125, 150, 175, and 200 mg L^{-1} and an initial solution pH of 6.5 during 20 h. The adsorption capacity of the walnut shell AC for all initial concentrations is shown in Fig. 5. The maximum adsorption capacity of CFX 243.13 mg g^{-1} was obtained at 200 mg L^{-1} initial concentration.

5.4. Adsorption isotherm

Fig. 6 shows the adsorption equilibrium isotherm of CFX onto walnut shell AC. The equilibrium data are fitted by two-parameter model of the Langmuir and Freundlich isotherm [29,30] and three-parameter model of the Sips and Toth isotherm [31,32] by using MATLAB. The validity of these models was evaluated using root mean square error (RMSE) which is defined as:

$$\text{RMSE} = \sqrt{\frac{\sum_{n=1}^n (q_{e,\text{exp}} - q_{e,\text{cal}})^2}{n}} \quad (14)$$

where n is the number of experimental data. The parameters, accuracy coefficient value, and RMSE for adsorption of CFX onto the walnut shell AC are presented in Table 2. As shown in Table 2, the best fitting

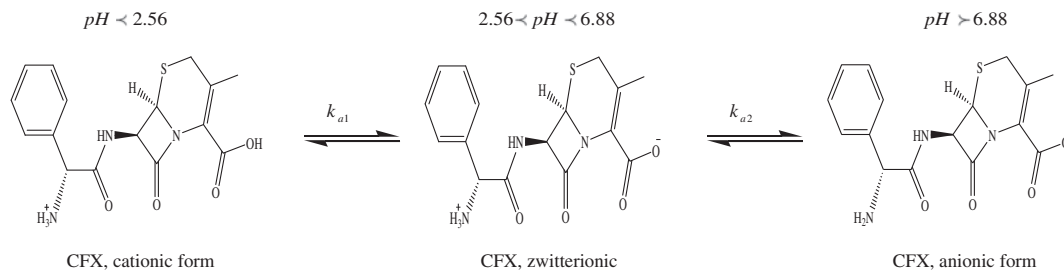


Fig. 4. Molecular structure of CFX and its ionic forms as a function of pH.

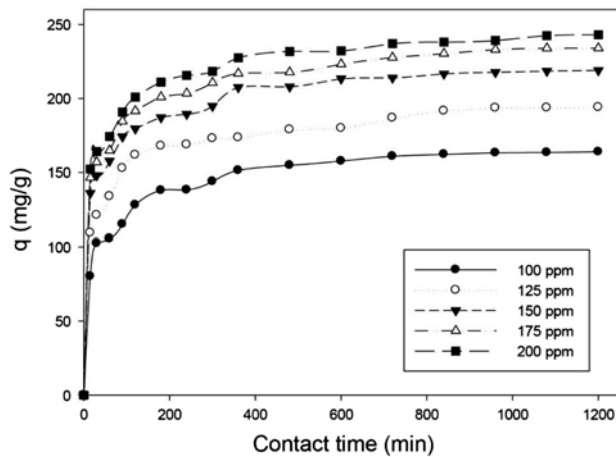


Fig. 5. Effect of contact time on adsorption of CFX on the walnut shell AC.

of experimental data for two and three-parameter isotherm models is achieved by the Freundlich and Toth models, respectively. The maximum adsorption capacity (q_{max}) of the walnut shell AC toward CFX was found to be 233.1 mg g^{-1} based on the Langmuir model. As it is shown in Table 3, the q_{max} obtained in this study is comparable with those reported in the literature for the adsorption of CFX and other pharmaceuticals onto different adsorbents.

5.5. Adsorbent characterization

It is found that the specific surface area, average pore diameter, and total pore volume of the walnut shell AC are $1452.1 \text{ m}^2 \text{ g}^{-1}$, 1.97 nm , and $0.7151 \text{ cm}^3 \text{ g}^{-1}$, respectively. The SEM analysis of the walnut shell AC adsorbent before and after CFX adsorption is illustrated in Fig. 7. This figure depicts a dramatic change in the structure of walnut shell AC after adsorption where the surface is covered with the CFX molecules. For determination of bonds in the synthesized adsorbent, before and after adsorption, the FTIR analysis was used. The FTIR spectrum of walnut

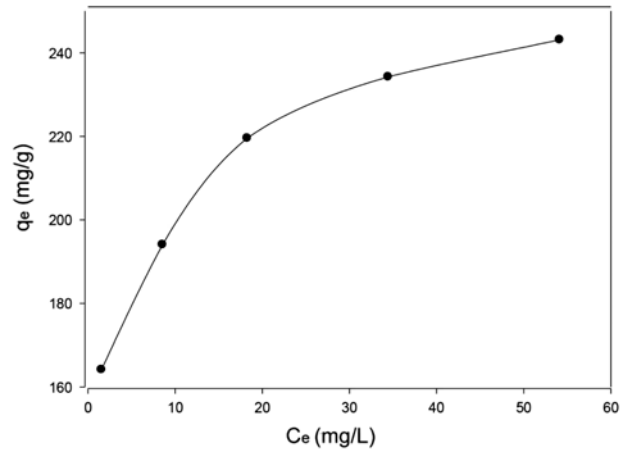


Fig. 6. Equilibrium data for adsorption of CFX on the walnut shell AC ($T = 30^\circ\text{C}$ and $C_0 = 150 \text{ mg L}^{-1}$).

Table 2

Isotherm model parameters, regression coefficients, and RMSE values for adsorption of CFX onto walnut shell AC

Isotherm model	Expression	Parameters
Langmuir	$q_e = \frac{q_m b C_e}{1 + b C_e}$	q_m (mg g^{-1}) = 233.1 b (L mg^{-1}) = 1.355 $R^2 = 0.8328$ RMSE = 15.17
Freundlich	$q_e = K_F C_e^{1/n}$	$K_F \left(\frac{(\text{mg/g})}{(1/\text{mg})^{-1/n}} \right) = 155.2$ $n = 8.772$ $R^2 = 0.9913$ RMSE = 3.459
Sips	$q_e = \frac{K_s C_e^{\beta_s}}{1 + \alpha_s C_e^{\beta_s}}$	K_s (L g^{-1}) = 172.29 α_s (L mg^{-1}) = 0.1141 q_m (mg g^{-1}) = 1,510 $\beta_s = 0.1322$ $R^2 = 0.9912$ RMSE = 4.272
Toth	$q_e = \frac{K_T C_e}{(a_T + C_e)^{1/t}}$	K_T (mg g^{-1}) = 155.1 a_T (mg g^{-1}) = 1.1×10^{-12} $t = 1.129$ $R^2 = 0.9913$ RMSE = 3.459

Table 3

Comparison of q_{\max} for the adsorption of CFX and other pharmaceuticals using different adsorbents

Adsorbent	Adsorbate	Activator	pH	q_{\max} (mg g ⁻¹)	Refs.
Graphene oxide	Tetracycline	–	3.6	313.00	[33]
Cattail fiber-carbon	Norfloxacin	H ₃ PO ₄	–	–	[34]
Walnut shell AC	Cephalexin	ZnCl ₂	6.5	233.10	This study
Activated carbon	Ciprofloxacin	H ₃ PO ₄	5.0	231.00	[35]
Commercial-carbon	Cephalexin	Steam	7.0	230.88	[10]
Commercial-carbon	Cephalexin	Steam	3.0	222.33	[13]
Graphene oxide	Oxytetracycline	–	3.6	212.00	[33]
A.L. seed pods-carbon	Cephalexin	KOH	7.0	137.02	[9]
		K ₂ CO ₃	7.0	118.08	
Carbon xerogel	Ciprofloxacin	–	5.0	112.00	[35]
Lotus stalks-carbon	Cephalexin	Cu(NO ₃) ₂	7.0	78.12	[12]
		Fe(NO ₃) ₂	8.5	75.12	
		H ₃ PO ₄	6.5	66.22	
Animal hairs-carbon	Acetaminophen	H ₃ PO ₄	–	61.80	[34]
Cattail fiber-carbon	Acetaminophen	H ₃ PO ₄	–	59.90	[34]
Amberlite XAD7-resin	Cephalexin	–	3.0	33.02	[13]

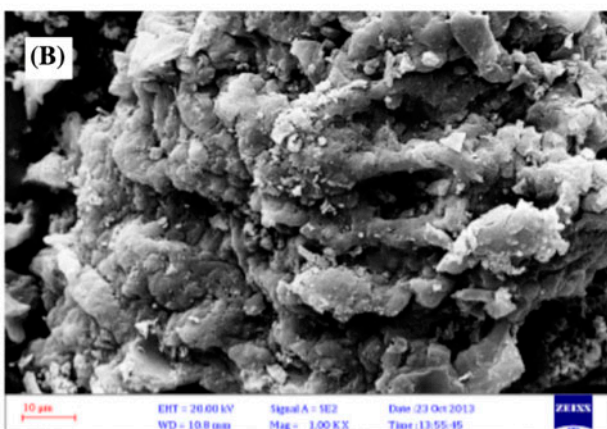
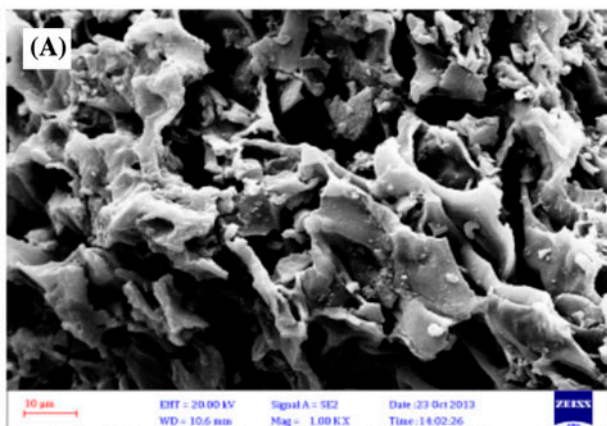


Fig. 7. SEM micrograph of walnut shell AC before (A) and after (B) CFX adsorption.

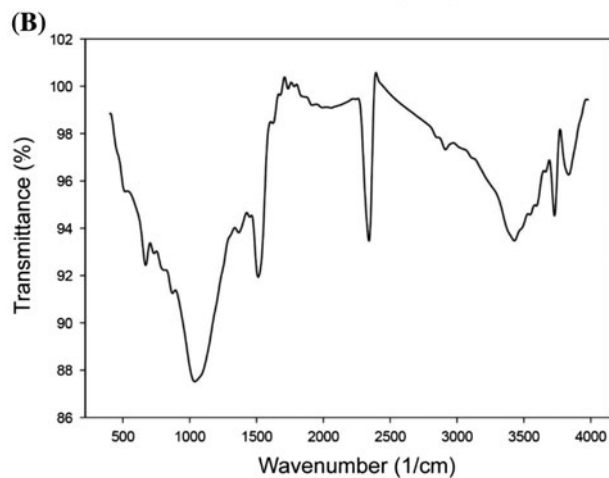
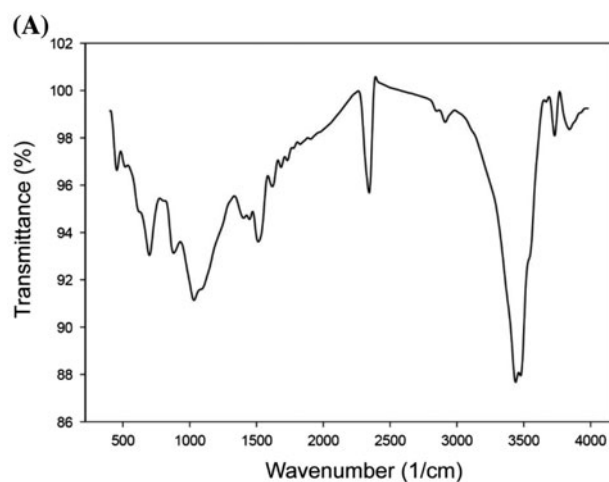


Fig. 8. FTIR spectra of walnut shell AC before (A) and after adsorption (B).

shell AC is demonstrated in Fig. 8. This figure shows peaks at $1,044\text{ cm}^{-1}$ (–C–O stretching), $1,525\text{ cm}^{-1}$ (–N–O stretch (strong, two bonds) nitro), $1,742\text{ cm}^{-1}$ (–C=O stretch and stretch (strong)), $2,355\text{ cm}^{-1}$ (–C≡C stretching), $2,924\text{ cm}^{-1}$ (–CH stretch (strong)), $3,451\text{ cm}^{-1}$ (–OH stretch, H-bonded), $3,742\text{ cm}^{-1}$ (–NH₂ stretching), and $3,853\text{ cm}^{-1}$ (NA) that are shifted to $1,050$, $1,024$, $1,748$, $2,353$, $2,926$, $3,440$, $3,741$, and $3,846\text{ cm}^{-1}$, respectively, after adsorption [26,36]. The peaks at 467 cm^{-1} (–OH bending), 710 cm^{-1} (–C–H bending and C–Cl stretch (strong)), 891 cm^{-1} (–C–H out-of-plane bending), $1,630\text{ cm}^{-1}$ (the olefinic $\nu(\text{C}=\text{C})$ absorptions), and $1,696\text{ cm}^{-1}$ (–C=O stretch (strong) amide) disappeared, while some new peaks are also detected at 683 cm^{-1} ($\gamma(\text{O–H})$ and C–Cl stretch (strong)) and $1,378\text{ cm}^{-1}$ (–N–O stretch (strong)) [36,37].

5.6. Results of the model

The Toth equilibrium isotherm was exploited in the model. Physical properties, namely porosity and skeletal density were measured $0.59\text{ cm}^3\text{ cm}^{-3}$ and 2 g cm^{-3} for the modified adsorbent, respectively. For estimation of the model parameter, effective diffusivity, comparison of the model and experiment was employed for the purpose of minimization of absolute average relative deviation (AARD). The value of $0.18 \times 10^{-9}\text{ m}^2\text{ s}^{-1}$ is the best value that fits the experimental data. The diffusion coefficient of CFX in pure water has been previously reported as $0.46 \times 10^{-9}\text{ m}^2\text{ s}^{-1}$ [38]. Corresponding diffusivity for the case of CFX in pure water can be calculated using the simple equation given by Wakao and Smith [39] which is:

$$D_e = \varepsilon_p^2 D_{AB} \quad (15)$$

The pertinent effective diffusivity for the case mentioned in this study corresponds to the value of $0.16 \times 10^{-9}\text{ m}^2\text{ s}^{-1}$. This value is slightly less than the evaluated value from the experimental one which may be either a result of the inherent underestimation of the Eq. (15) or simplifying assumption of spherical adsorbent with uniform sizes (average size in the mentioned mesh was used). The model and experimental results are compared in Fig. 9. The adsorption decay curves are converging to the marked horizontal asymptotes, which indicate the equilibrium state described in Section 2.1. This convergence to equilibrium state validates the accuracy of the numerical procedure. The pore and solid phase concentration profiles are demonstrated for the case of $C_0 = 150\text{ mg L}^{-1}$ in Fig. 10(A) and (B), respectively.

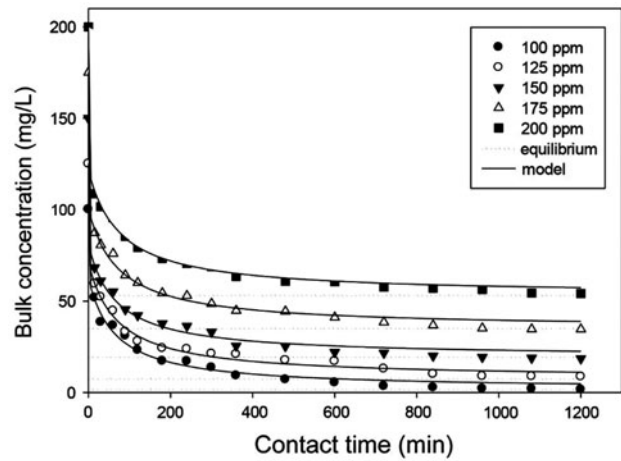


Fig. 9. Comparison of the model and experiment.

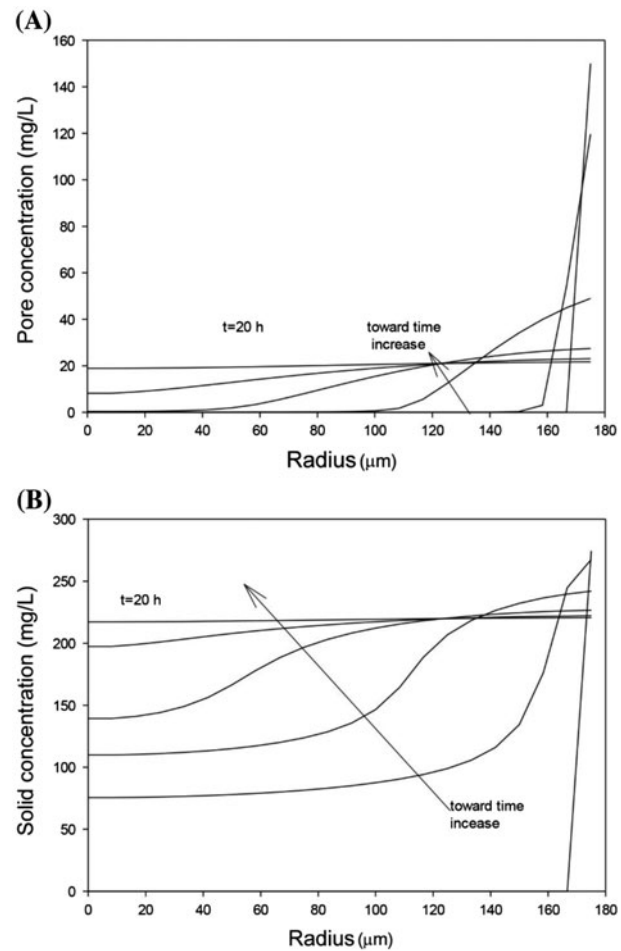


Fig. 10. Concentration profiles at different times: pore concentration profiles (A) and solid concentration profiles (B) ($T = 30^\circ\text{C}$ and $C_0 = 150\text{ mg L}^{-1}$).

6. Conclusion

The present study has been conducted in two experimental and modeling sections. In the first step, AC was prepared from chemical activation of walnut shell in the presence of ZnCl_2 . Then, the adsorptive performance of the walnut shell AC in the removal of CFX from aqueous solution was investigated. In the next section, a model was developed to simulate the dynamics of the adsorption process. The main results based on the experimental and theoretical studies, can be summarized as follows:

- (1) The maximum CFX adsorption capacity at the adsorbent dosage of 0.6 g L^{-1} and the initial pH value of 6.5 was 233.1 mg g^{-1} based on the Langmuir model. Moreover, the kinetics shows that a contact time of about 20 h is sufficient enough to reach the equilibrium state.
- (2) It was found that the Freundlich and Toth models provide the best fit to the experimental data among two and three-parameter models, respectively.
- (3) Using the experimental data, effective macropore diffusivity was estimated. The value of $0.18 \times 10^{-9} \text{ m}^2 \text{ s}^{-1}$ is the best value that fits the experimental data. This value appears to be slightly more than the value predicted by Wakao and Smith equation. The model showed perfect agreement with experimental data.

Acknowledgments

The authors are really thankful to editor and anonymous reviewers of the journal of Desalination and Water Treatment for their precious comments and suggestions on this article. The authors would also like to acknowledge Mr Ehsan Sadeghi Pouya and Mr Seyed Adel Hosseini for his unwavering support.

References

- [1] V. Gabet-Giraud, C. Miège, J.M. Choubert, S.M. Ruel, M. Coquery, Occurrence and removal of estrogens and beta blockers by various processes in wastewater treatment plants, *Sci. Total Environ.* 408(19) (2010) 4257–4269.
- [2] A. Ziylan, N.H. Ince, The occurrence and fate of anti-inflammatory and analgesic pharmaceuticals in sewage and fresh water: Treatability by conventional and non-conventional processes, *J. Hazard. Mater.* 187(1) (2011) 24–36.
- [3] C. Watts, D. Maycoak, M. Crane, J. Fawell, Desk based review of current knowledge on pharmaceuticals in drinking water and estimation of potential levels, Final Report to Defra Project Code: CSA 7184/WT02046/DWI70/2/213, 2007.
- [4] I. Turku, T. Sainio, E. Paatero, Thermodynamics of tetracycline adsorption on silica, *Environ. Chem. Lett.* 5(4) (2007) 225–228.
- [5] H. Kim, Y.S. Hwang, V.K. Sharma, Adsorption of antibiotics and iopromide onto single-walled and multi-walled carbon nanotubes, *Chem. Eng. J.* 255 (2014) 23–27.
- [6] Y. Zhao, J. Geng, X. Wang, X. Gu, S. Gao, Tetracycline adsorption on kaolinite: pH, metal cations and humic acid effects, *Ecotoxicology* 20(5) (2011) 1141–1147.
- [7] P. Liao, Z. Zhan, J. Dai, X. Wu, W. Zhang, K. Wang, S. Yuan, Adsorption of tetracycline and chloramphenicol in aqueous solutions by bamboo charcoal: A batch and fixed-bed column study, *Chem. Eng. J.* 228 (2013) 496–505.
- [8] M.E. Parolo, M.J. Avena, G.R. Pettinari, M.T. Baschini, Influence of Ca^{2+} on tetracycline adsorption on montmorillonite, *J. Colloid Interface Sci.* 368(1) (2012) 420–426.
- [9] M.J. Ahmed, S.K. Theydan, Adsorption of cephalixin onto activated carbons from *Albizia lebbek* seed pods by microwave-induced KOH and K_2CO_3 activations, *Chem. Eng. J.* 211 (2012) 200–207.
- [10] M. Dutta, R. Baruah, N. Dutta, A. Ghosh, The adsorption of certain semi-synthetic cephalosporins on activated carbon, *Colloids Surf. A: Physicochem. Eng. Aspects* 127(1) (1997) 25–37.
- [11] W. Liu, H. Xie, J. Zhang, C. Zhang, Sorption removal of cephalixin by HNO_3 and H_2O_2 oxidized activated carbons, *Sci. China Chem.* 55(9) (2012) 1959–1967.
- [12] H. Liu, W. Liu, J. Zhang, Y. Li L. Ren, Y. Li, C. Zhang, Removal of cephalixin from aqueous solution by original and Cu(II)/Fe(III) impregnated activated carbons developed from lotus stalks kinetics and equilibrium studies, *Sci. China Chem.* 185(2) (2011) 1528–1535.
- [13] N. Dutta, M.D. Saikia, Adsorption equilibrium of 7-aminodeacetoxy cephalosporanic acid–cephalexin mixture onto activated carbon and polymeric resins, *Indian J. chem. Technol.* 12(3) (2005) 296–303.
- [14] V.O. Njoku, M. Azharul Islam, M. Asif, B.H. Hameed, Preparation of mesoporous activated carbon from coconut frond for the adsorption of carbofuran insecticide, *J. Anal. Appl. Pyrolysis* 110 (2014) 172–180.
- [15] Y. Zhang, X.-L. Song, S.-T. Huang, B.-Y. Geng, C.-H. Chang, I.-Y. Sung, Adsorption of nitrate ions onto activated carbon prepared from rice husk by NaOH activation, *Desalin. Water Treat.* 52(25–27) (2014) 4935–4941.
- [16] G. Karaçetin, S. Sivrikaya, M. Imamoğlu, Adsorption of methylene blue from aqueous solutions by activated carbon prepared from hazelnut husk using zinc chloride, *J. Anal. Appl. Pyrolysis* 110 (2014) 270–276.
- [17] L. Huang, M. Wang, C. Shi, J. Huang, B. Zhang, Adsorption of tetracycline and ciprofloxacin on activated carbon prepared from lignin with H_3PO_4 activation, *Desalin. Water Treat.* 52(13–15) (2014) 2678–2687.
- [18] J. Crank, *The Mathematics of Diffusion*, second ed., Clarendon Press, Oxford, 1979.
- [19] D.W.G. H. R. Perry, *Perry's Chemical Engineering Handbook: Adsorption and Ion Exchange*, seventh ed., McGraw-Hill, New York, NY, 1997.
- [20] J.T. Hsu, T.-L. Chen, Theoretical analysis of the asymmetry in chromatographic peaks, *J. Chromatogr. A* 404 (1987) 1–9.

- [21] P.R. Kasten, L. Lapidus, N.R. Amundson, Mathematics of adsorption in beds. V. Effect of intra-particle diffusion in flow systems in fixed beds, *J. Phys. Chem.* 56(6) (1952) 683–688.
- [22] I.-S. Park, Frequency response of the adsorption vessel loaded with inert core adsorbents, *Korean J. Chem. Eng.* 22(6) (2005) 960–963.
- [23] A. Rasmuson, Exact solution of a model for diffusion and transient adsorption in particles and longitudinal dispersion in packed beds, *AIChE J.* 27(6) (1981) 1032–1035.
- [24] T.M. Alslaibi, I. Abustan, M.A. Ahmad, A.A. Foul, Comparison of activated carbon prepared from olive stones by microwave and conventional heating for iron (II), lead (II), and copper (II) removal from synthetic wastewater, *Environ. Prog. Sustain. Energy* 33 (4) (2014) 1074–1085.
- [25] G. McKay, Solution to the homogeneous surface diffusion model for batch adsorption systems using orthogonal collocation, *Chem. Eng. J.* 81(1) (2001) 213–221.
- [26] J. Yang, K. Qiu, Preparation of activated carbons from walnut shells via vacuum chemical activation and their application for methylene blue removal, *Chem. Eng. J.* 165(1) (2010) 209–217.
- [27] W. Cai, L. Tan, J. Yu, M. Jaroniec, X. Liu, B. Cheng, F. Verpoort, Synthesis of amino-functionalized mesoporous alumina with enhanced affinity towards Cr (VI) and CO₂, *Chem. Eng. J.* 239 (2014) 207–215.
- [28] M.S. Reddy, L. Sivaramakrishna, A.V. Reddy, The use of an agricultural waste material, Jujuba seeds for the removal of anionic dye (Congo red) from aqueous medium, *J. Hazard. Mater.* 203 (2012) 118–127.
- [29] H.M.F. Freundlich, Over the adsorption in solution, *J. Phys. Chem. A* 57 (1906) 385–471.
- [30] I. Langmuir, The constitution and fundamental properties of solids and liquids. II. Liquids. 1, *J. Am. Chem. Soc.* 39 (1917) 1848–1906.
- [31] R. Sips, Combined form of Langmuir and Freundlich equations, *J. Chem. Phys.* 16 (1948) 490–495.
- [32] J. Toth, State equations of the solid gas interface layer, *Acta Chem. Acad. Hung.* 69 (1971) 311–317.
- [33] Y. Gao, Y. Li, L. Zhang, H. Huang, J. Hu, S.M. Shah, X. Su, Adsorption and removal of tetracycline antibiotics from aqueous solution by graphene oxide, *J. Colloid Interface Sci.* 368(1) (2012) 540–546.
- [34] L. Hai, W. Ning, P. Cheng, J. Zhang, Y. Wang, C. Zhang, Evaluation of animal hairs-based activated carbon for sorption of norfloxacin and acetaminophen by comparing with cattail fiber-based activated carbon, *J. Anal. Appl. Pyrolysis* 101 (2013) 156–165.
- [35] S. Carabineiro, T. Thavorn-Amornsri, M. Pereira, P. Serp, J. Figueiredo, Comparison between activated carbon, carbon xerogel and carbon nanotubes for the adsorption of the antibiotic ciprofloxacin, *Catal. Today* 186(1) (2012) 29–34.
- [36] S. Reddy, L. Sivaramakrishna, A. Varada Reddy, The use of an agricultural waste material, Jujuba seeds for the removal of anionic dye (Congo red) from aqueous medium, *J. Hazard. Mater.* 203 (2012) 118–127.
- [37] T. Yang, A.C. Lua, Textural and chemical properties of zinc chloride activated carbons prepared from pistachio-nut shells, *Mater. Chem. Phys.* 100(2) (2006) 438–444.
- [38] T. Seki, M. Okamoto, O. Hosoya, D. Aiba, K. Morimoto, K. Juni, Effect of chondroitin sulfate on the diffusion coefficients of drugs in aqueous solutions, *STP Pharma. Sci.* 13(3) (2003) 215–218.
- [39] N. Wakao, J. Smith, Diffusion in catalyst pellets, *Chem. Eng. Sci.* 17(11) (1962) 825–834.